Density of States of quasi-equilibrium Bose-Einstein condensed magnons in YIG

Maxime Jonker

June 18, 2014

Bachelor Thesis

Supervisor:

Dr. R.A. Duine

Institute for Theoretical Physics
Utrecht University

Abstract

The experimental observation of quasi-equilibrium Bose-Einstein condensation of magnons in yttrium iron garnet at room temperature was first reported by Demokritov *et al*. in 2006 [1]. These authors used their experimental data to obtain a fit for the density of states. In this Thesis we examine the density of states from a theoretical perspective. A theoretical model for magnons in yttirum iron garnet is used. From this model a dispersion relation follows, which is used to obtain the density of states. This is first done by approximating the dispersion around the minimum, allowing for an analytical computation of the density of states. Subsequently an expression for the density of states in the form of an integral over the wave number k is obtained from the model without any further approximations. This integral will have to be evaluated numerically, which is left for future work.

Contents

1 Introduction

In 2006 Demokritov *et al.* were the first to report the observation of quasi-equilibrium Bose-Einstein condensation in a gas of magnons at room temperature [1]. This is interesting for several reasons, first of which is the fact that Bose-Einstein condensation in itself is an interesting phenomenon. Bose-Einstein condensation is a macroscopic occupation of the single-particle ground state energy, which allows for the observation of quantum effects on a macroscopic scale, whereas the quantum nature of matter usually remains hidden from the macroscopic world, being only detectable on subatomic distances. Secondly, the fact that the observation was made at room temperature distinguished it from observations of Bose-Einstein in cold atomic gasses that had been reported before. Up to then the temperature had to be lowered to the ultracold, i.e. in the order of nanokelvins, regime, in order to meet the conditions for Bose-Einstein condensation [2]. This was changed by the technique applied in Ref.[1], which consisted of parametric pumping of magnons in a material called yttrium iron garnet (YIG). Due to its properties this material allowed the density of the magnons to be increased sufficiently to reach Bose-Einstein condensation, even at room temperature.

This brings us to the next remarkable aspect: the particles that formed the Bose-Einstein condensate were actually not particles but quasiparticles, i.e. collective excitations that can be quantized and treated as if they are weakly interacting particles. Magnons, also referred to as spin waves, make up collective excitations in magnetic materials and do behave like weakly interacting bosons, as long as the temperature is well below the critical temperature for the ordered state. In thermal equilibrium magons have a chemical potential equal to zero because their total particle number is not conserved. As we will see shortly, this implies that they cannot form a Bose-Einstein condensate under normal circumstances. In the experiment, however, they were in a so-called quasi-equilibrium with a non-zero chemical potential, which made the formation of a Bose-Einstein condensate possible.

In order to interpret the experimental data, which consisted of measured scattering intensities over a spectrum of frequencies (corresponding to energy levels), the intensity had to be related somehow to the distribution of the magnons. This was done by means of the density of states, which relates the total number of particles or particle density to the distribution function, describing the average occupation number of each state at a given energy. The density of states is an important concept, usually encountered when one wants to calculate the total particle density in order to derive other thermodynamic properties. The density of states can in principle be computed from the dispersion relation, i.e. the relation between energy levels and corresponding quantum numbers, or, equivalently, frequencies and corresponding wave vectors. When the dispersion relation is relatively simple, the density of states can usually be computed analytically.

However, in Ref.[1], the density of states was not calculated but obtained from a fit of the experimental data to the distribution function. The main goal of this thesis is to find an expression for the density of states by taking on a theoretical approach and using a model describing magnon interactions in YIG.

We will start, however, with discussing the theory behind Bose-Einstein condensation in Section 2, by deriving the Bose-Einstein distribution function

and finding out what the conditions are for Bose-Einstein condensation to occur. Section 3 is devoted to a description of magnons, both in a semiclassical way and a quantum mechanical way. In Section 4 the experiment will be discussed, including the experimental set-up and the relevant results. In Section 5 we will discuss a theoretical model describing magnons in YIG that provides a more accurate expression for the dispersion relation of the magnons. From this dispersion relation we will try to obtain an expression for the density of states. Analytical and numerical results are then presented. Eventually we will finish with a conclusion in Section 6.

2 Bose-Einstein condensation

In this section we will give a theoretical account of Bose-Einstein condensation by means of the Bose-Einstein distribution function (see, for example, Ref.[3]). We will see that Bose-Einstein condensation occurs under specific conditions, when either a critical temperature or a critical density is reached. Furthermore, we will give a definition of the density of states and see how it plays a role in relating the distribution function to the particle density.

2.1 Theory of Bose-Einstein condensation

Bose-Einstein condensation is one of the most striking phenomena resulting from the quantum nature of matter. It is a state of matter in which a macroscopic number of identical particles occupy the single-particle ground state. In this manner a collective quantum state is formed, causing quantum effects to become visible on a macroscopic scale and giving rise to fascinating properties such as superfluidity [3]. To understand the theory behind Bose-Einstein condensation we need to examine Bose-Einstein statistics. Let us therefore first derive the Bose-Einstein distribution function, departing from the grand-canonical partion function of a gas of identical particles in the thermodynamic limit. This partition function reads:

$$Z = \sum_{N=0}^{\infty} e^{\beta\mu N} \sum_{\{n_{\mathbf{k}}\}} e^{-\beta \sum_{\mathbf{k}} n_{\mathbf{k}}\epsilon_{\mathbf{k}}}, \tag{1}$$

where the inner sum is over the set of occupation numbers $n_{\mathbf{k}}$ that is restricted by the condition $\sum_{\mathbf{k}} n_{\mathbf{k}} = N$, with N the total particle number. However, since N itself runs from zero to infinity, we can rewrite Eq.(1) as a sum over the set $\{n_{\mathbf{k}}\}$, that is no longer restricted:

$$Z = \sum_{\{n_{\mathbf{k}}\}} e^{-\beta \sum_{\mathbf{k}} (n_{\mathbf{k}}\epsilon_{\mathbf{k}} - n_{\mathbf{k}}\mu)} = \sum_{\{n_{\mathbf{k}}\}} \prod_{\mathbf{k}} e^{-\beta n_{\mathbf{k}}(\epsilon_{\mathbf{k}} - \mu)} \tag{2}$$

$$= \sum_{n_1} \sum_{n_2} \sum_{n_3} \cdots e^{-\beta n_1(\epsilon_1 - \mu)} e^{-\beta n_2(\epsilon_2 - \mu)} e^{-\beta n_3(\epsilon_3 - \mu)} \cdots \tag{3}$$

$$= \prod_{\mathbf{k}} \sum_{n_{\mathbf{k}}} e^{-\beta n_{\mathbf{k}}(\epsilon_{\mathbf{k}} - \mu)} = \prod_{\mathbf{k}} Z_{\mathbf{k}}. \tag{4}$$

Before proceeding we should point out that n_k denotes the occupation number for a state with wavevector $\mathbf{k}$. In the case of fermions, the Pauli principle tells us that this number can only take on the values one and zero. When we are

dealing with bosons, however, $n_{\mathbf{k}}$ runs from zero to infinity. Performing the sum over $n_{\mathbf{k}}$ we find for bosons:

$$Z = \prod_{\mathbf{k}} \sum_{n_{\mathbf{k}}=0}^{\infty} \left(e^{-\beta(\epsilon_{\mathbf{k}}-\mu)}\right)^{n_{\mathbf{k}}} = \prod_{\mathbf{k}} \left(1 - e^{-\beta(\epsilon_{\mathbf{k}}-\mu)}\right)^{-1}. \tag{5}$$

The total energy E of the system is given by

$$E = -\frac{\partial}{\partial\beta} \ln Z + \mu N = -\frac{\partial}{\partial\beta} \sum_{\mathbf{k}} \ln\left(1 - e^{-\beta(\epsilon_{\mathbf{k}}-\mu)}\right) + \mu N \tag{6}$$

$$= \sum_{\mathbf{k}} \frac{1}{e^{\beta(\epsilon_{\mathbf{k}}-\mu)} - 1} (\epsilon_{\mathbf{k}} - \mu) + \mu N. \tag{7}$$

But also

$$E = \sum_{\mathbf{k}} \langle n_{\mathbf{k}} \rangle \, \epsilon_{\mathbf{k}} \quad \text{and} \quad N = \sum_{\mathbf{k}} \langle n_{\mathbf{k}} \rangle \,, \tag{8}$$

where $\langle n_{\mathbf{k}} \rangle$ denotes the average occupation number of a state with wave vector $\mathbf{k}$. From Eq.(7) and Eq.(8) we deduce that

$$\langle n_{\mathbf{k}} \rangle = \frac{1}{e^{\beta(\epsilon_{\mathbf{k}}-\mu)} - 1} = N_{BE}(\epsilon_{\mathbf{k}}), \tag{9}$$

is the Bose-Einstein distribution function. From Eq.(9) we see that the chemical potential μ cannot be greater than $\epsilon_{\mathbf{k}}$, to prevent the occupation number from taking on a negative value. This means that $\mu \leq \epsilon_{min}$, with ϵ_{min} denoting the single-particle ground state. The case where $\mu = \epsilon_{min}$ represents the critical point for the occurrence of Bose-Einstein condensation. At this point either the particle density exceeds a critical value or the temperature is decreased to a critical temperature. This can be understood by examining the expression for the total number of particles N:

$$N = \sum_{\mathbf{k}} \frac{1}{e^{\beta(\epsilon_{\mathbf{k}}-\mu)} - 1}. \tag{10}$$

When the total particle number is held constant and the temperature is decreased, the chemical potential will increase until it is equal to ϵ_{min}. On the other hand, if the temperature is constant, the particle number, or density, will have to be increased to a critical density in order to let μ reach its maximum value. When this happens, the additional particles can not be accomodated anymore in the states as described by the Bose-Einstein distribution function. The result is that a large fraction of the total particle number will occupy the single-particle ground state. It is important to stress that Bose-Einstein condensation can only occur in a system of bosonic particles, as opposed to fermions. The derivation of the Bose-Einstein distribution function was based on the fact that the occupation number for bosons can take on any positive integer value, whereas that for fermions is never larger than one due to the Pauli exclusion principle, stating that two or more fermions cannot occupy the same state. Accordingly, it would never be possible for fermions to collectively occupy the single-particle groundstate.

2.2 Critical density and density of states

The critical density $n_c(T)$ as a function of temperature can be obtained by setting μ equal to ϵ_{min} in Eq.(10), since at the critical density all the particles will still be precisely accomodated in the excited states and the fraction occupying the ground state is still negligable compared to N. The sum can then be converted to an integral over $\mathbf{k}$ by making the substitution

$$\sum_{\mathbf{k}} \to \frac{L^3}{(2\pi)^3} \int \mathrm{d}\mathbf{k}\,, \tag{11}$$

where L^3 is the volume of the system and, as usual, the wavevector components are quantized according to $k_i = 2\pi n_i/L$. Treating k as a continuous variable is valid when the spacing between the energy states is much smaller than the thermal energy or when $L \to \infty$. Hence, we obtain the following expression for the critical particle density:

$$n_c = \int \frac{\mathrm{d}\mathbf{k}}{(2\pi)^3} \frac{1}{e^{\beta(\epsilon_{\mathbf{k}} - \epsilon_{min})}}. \tag{12}$$

This integral can be converted to an integral over energy ϵ in the following way:

$$\int \frac{\mathrm{d}\mathbf{k}}{(2\pi)^3} \frac{1}{e^{\beta(\epsilon_{\mathbf{k}} - \epsilon_{min})}} = \int \frac{\mathrm{d}\mathbf{k}}{(2\pi)^3} \int \mathrm{d}\epsilon\ \delta(\epsilon - \epsilon_{\mathbf{k}})\ \frac{1}{e^{\beta(\epsilon - \epsilon_{min})}} \tag{13}$$

$$= \int \mathrm{d}\epsilon\, D(\epsilon)\, \frac{1}{e^{\beta(\epsilon - \epsilon_{min})}}, \tag{14}$$

where we introduced the density of states $D(\epsilon)$:

$$D(\epsilon) = \int \frac{\mathrm{d}\mathbf{k}}{(2\pi)^3}\ \delta(\epsilon - \epsilon_{\mathbf{k}}). \tag{15}$$

We see here that the density of states is required in order to evaluate n_c. More generally, the density of states can be used to convert sums over discrete quantum numbers, such as wave vectors, to integrals over the energy ϵ. When the dispersion relation, i.e. the relation between energy or, equivalently, frequency and wave vector is known, that is, when one has an expression for $\epsilon_{\mathbf{k}}$ as a function of $\mathbf{k}$, the density of states can in principle be calculated. Another way to define the density of states is by the relation

$$D(\epsilon) = \frac{\partial}{\partial \epsilon} N(\epsilon)\,, \tag{16}$$

where $N(\epsilon)$ is the total number of states with energy $\leq \epsilon$. As we will see also in following sections, the importance of the density of states lies in the fact that it relates the distribution function to the total particle density. However, before we come to concrete applications of this, we will first take a closer look at magnons and find a theoretical description of these boson-like quasiparticles.

3 Magnons

Before we come to discuss magnon Bose-Einstein condensation, an understanding of the notion of magnons is required. As mentioned previously, magnons do not consist of ordinary matter but are quasiparticles. In this section we will see what this precisely means, by giving several descriptions of magnons, varying from rather classical and intuitive to purely quantum mechanical.

3.1 What are magnons?

There are several ways to approach the concept of magnons, but one way to define them is as elementary excitations in ordered magnetic materials, an idea first suggested by Bloch [4]. Intuitively this corresponds to the classical picture of a chain of spins deviating slightly from their ground state orientations, with these deviations propagating trough the material in a wave-like manner, forming so-called spin waves. This idea is illustrated in Figure 1. It is analogous to elementary lattice vibrations caused by the oscillations of the atoms around their equilibrium position and propagating through the material in the form of waves. Spins, however, do not have a classical analogue, which is why the picture of spin waves presented here is not completely accurate. Taking their quantum mechanical nature into account, the spin waves can be quantized, with a magnon being the quantum of a spin wave, analogously to the phonon being a quantized lattice vibration. A purely quantum mechanical approach to magnons makes use of the Holstein-Primakoff transformation, which is based on second quantization and in which magnons are represented by bosonic operators, replacing the spin raising and lowering operators. A magnon can then be thought of as one quantum of spin reversal, spread over the lattice [6]. In the following paragraphs we will examine both approaches, applied to the simple Heisenberg Hamiltonian, describing a system of interacting spins in a magnetic material:

$$H = -J \sum_{\langle ij \rangle} \mathbf{S_i} \cdot \mathbf{S_j} \,, \tag{17}$$

where the sum is over all pairs i and j of lattice sites, $\mathbf{S}_i$ denotes the spin at lattice site i, and J is the exchange coupling, that has a positive value for ferromagnets and ferrimagnets, implying the energy is minimized when all spins point along the same direction.

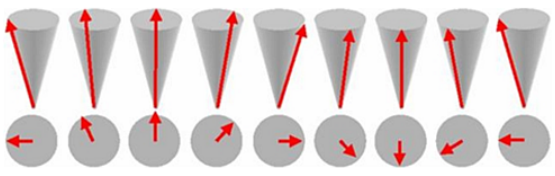

Figure 1: Spin waves depicted as vectors precessing around their ground state orientation. Taken from Ref.[5].

3.2 Semiclassical approach

In order to gain a physical interpretation of magnons it is instructive to study them from a (semi)classical approach. In this approach we will treat the magnons as spin waves in a one-dimensional chain of spins pointing along the z-axis, separated by a distance a. Starting from the Heisenberg exchange Hamiltonian, Eq.(1), we use Eherenfest's theorem to write down the classical equations of motion:

$$\frac{\mathrm{d}}{\mathrm{d}t}\langle \mathbf{S}_i \rangle = -\frac{i}{\hbar}\langle [\mathbf{S}_i, H] \rangle. \tag{18}$$

Considering only nearest neighbour interactions and taking the coupling J to be positive we obtain

$$\frac{\mathrm{d}}{\mathrm{d}t}\left\langle S_i^x \right\rangle \;=\; J\left\langle \left[S_i^y \left(S_{i-1}^z + S_{i+1}^z \right) - S_i^z \left(S_{i-1}^y + S_{i+1}^y \right) \right] \right\rangle, \tag{19}$$

where we used the commutation relations for spin operators,

$$[S_i^x, S_j^y] = iS_i^z\delta_{ij}, \quad [S_i^y, S_j^z] = iS_i^x\delta_{ij}, \quad [S_i^z, S_j^x] = iS_i^y\delta_{ij}.$$

The other two components of $\frac{\mathrm{d}}{\mathrm{d}t}\langle \mathbf{S} \rangle$ follow by cyclic permutation.

We now consider small deviations of the spin $\mathbf{S}$ from the z-axis, such that $S^z \approx S, \quad S^x, S^y \ll S$. This leads to

$$\frac{\mathrm{d}}{\mathrm{d}t}S_i^x \;=\; SJ\left(2S_i^y - S_{i-1}^y - S_{i+1}^y\right), \tag{20}$$

$$\frac{\mathrm{d}}{\mathrm{d}t}S_i^y \;=\; -SJ\left(2S_i^x - S_{i-1}^x - S_{i+1}^x\right). \tag{21}$$

Taking as an Ansatz

$$\begin{aligned} S_j^x = Ae^{ikR_j - i\omega t} \;&=\; Ae^{ikja - i\omega t}, \\ S_j^y = Be^{ikR_j - i\omega t} \;&=\; Be^{ikja - i\omega t}, \end{aligned}$$

and plugging these into Eq.(20) and Eq.(21), we find the following equations

$$-i\omega tA = 2SJB(1-\cos(ka)), \qquad -i\omega tB = -2SJA(1-\cos(ka)). \tag{22}$$

Solving these amounts to finding the zeros of

$$\det \begin{vmatrix} i\omega & 2SJ(1-\cos(ka)) \\ 2SJ(1-\cos(ka)) & -i\omega \end{vmatrix},$$

which leads us to the expression $\omega^2 = \left[\, 2SJ\left(1-\cos(ka)\right)\right]^2$ and, hence, the dispersion relation

$$\omega_k \;=\; 2SJ\left(1-\cos(ka)\right). \tag{23}$$

We thus find that we can picture magnons as spin waves, with each spin slightly tilted and precessing around the z-axis with frequency ω_k. For future reference

we note that the dispersion relation is quadratic for small wavenumbers k:

$$\omega_k \simeq SJ\,(ka)^2, \quad (ka \ll 1). \tag{24}$$

3.3 Holstein-Primakoff transformation

We will now derive the dispersion relation for magnons in a two dimensional lattice structure using the so-called Holstein-Primakoff transformation, in which the spin operators are replaced by bosonic creation and annihillation operators [7]. Let us first rewrite the Hamiltonian in terms of the spin raising and lowering operators S^+ and S^- by making use of the relations

$$S^+ = S^x + iS^y, \qquad S^- = S^x - iS^y,$$

$$S^x = \frac{S^+ + S^-}{2}, \qquad S^y = \frac{S^+ - S^-}{2i},$$

so that the Hamiltonian takes the form

$$H = -J \sum_{\langle ij \rangle} S_i^z\, S_j^z + \frac{1}{2}\,(S_i^+\, S_j^- + S_i^-\, S_j^+). \tag{25}$$

We now introduce the new operators $a^\dagger, a$:

$$\begin{aligned} S_i^+ &= \sqrt{2S}\,\sqrt{1 - a_i^\dagger a_i/2S}\,a_i\,, \\ S_i^- &= \sqrt{2S}\,a_i^\dagger\,\sqrt{(1 - a_i^\dagger a_i/2S}\,, \end{aligned} \tag{26}$$

so that a and $a^\dagger$ obey the standard commutation relation for bosonic operators: $[a_i, a_j^\dagger] = \delta_{ij}$. Next, we expand the square roots in Eq.(26) in powers of $1/S$, which is justified when the spin S is relativey large and fluctuations are small. When keeping only the lowest order terms we find

$$S_i^+ \simeq \sqrt{2S}\,a_i\,, \quad S_i^- \simeq \sqrt{2S}\,a_i^\dagger\,, \quad S_i^z \simeq S - a_i^\dagger a_i. \tag{27}$$

We see that the spin raising and lowering operators correspond to the boson annihilation and creation operators, respectively. This means that the creation of one magnon reduces the value of S^z by 1, which implies that magnons carry one $\hbar$ spin angular momentum. By inserting the expressions in Eq.(27) into our Hamiltonian, Eq.(25), we obtain the non-interacting spin wave Hamiltonian:

$$H = -J \sum_{\langle ij \rangle} (S - a_i^\dagger a_i)\,(S - a_j^\dagger a_j) + S\,(a_i^\dagger a_j + a_i a_j^\dagger) \tag{28}$$

$$\approx -JN(N-1)S^2 - JS \sum_{\langle ij \rangle} -2a_i^\dagger a_i + a_i^\dagger a_j + a_i a_j^\dagger + O(a^4) \tag{29}$$

$$= -JN(N-1)S^2 - JS \sum_{\langle ij \rangle} -2a_i^\dagger a_i + 2a_i^\dagger a_j + O(a^4). \tag{30}$$

Next, we perform a Fourier transform on the operators:

$$a_i = \frac{1}{\sqrt{N}} \sum_{\mathbf{k}} e^{i\mathbf{k}\cdot\mathbf{R_i}}, \qquad a_i^\dagger = \frac{1}{\sqrt{N}} \sum_{\mathbf{k}} e^{-i\mathbf{k}\cdot\mathbf{R_i}}, \tag{31}$$

where the sums are over two dimensional wave vectors $\mathbf{k}$ and $\mathbf{R_i}$ is a two dimensional vector denoting the position of lattice site i. If we choose our lattice to lie in the x, y-plane, $\mathbf{k} = k_x\hat{\mathbf{x}} + k_y\hat{\mathbf{y}}$ and $\mathbf{R}_i = m_i a\hat{\mathbf{x}} + n_i a\hat{\mathbf{y}}$, where a is the lattice constant and m and n are integers. Considering again only interactions between neighbouring lattice sites, we obtain:

$$\begin{aligned}\sum_{\langle ij\rangle} a_i^\dagger a_j \;=\; \frac{1}{2} \sum_{m,n} \frac{1}{N} \sum_{\mathbf{k},\mathbf{k'}} a_{\mathbf{k}}^\dagger a_{\mathbf{k'}}\, e^{-i(k_x ma + k_y na)} \big[& e^{i(k'_x(m+1)a + k'_y a)} + e^{i(k'_x(m-1)a + k'_y a)} \\ & + e^{i(k'_x ma + k'_y(n+1)a)} + e^{i(k'_x ma + k'_y(n-1)a)} \big]\end{aligned}$$

$$\begin{aligned}
&= \frac{1}{2} \sum_{\mathbf{k},\mathbf{k'}} a_{\mathbf{k}}^\dagger a_{\mathbf{k'}}\, \frac{1}{N} \sum_{m,n} \big[e^{ina(k'_y - k_y)} e^{ima(k'_x - k_x)} \big(e^{ik'_x a} + e^{-ik'_x a} \big) + e^{ima(k'_x - k_x)} e^{ina(k'_y - k_y)} \big(e^{ik'_y a} + e^{-ik'_y a} \big) \big] \\
&= \frac{1}{2} \sum_{\mathbf{k},\mathbf{k'}} a_{\mathbf{k}}^\dagger a_{\mathbf{k'}}\, \delta_{\mathbf{k},\mathbf{k'}} \left(e^{ik'_x a} + e^{-ik'_x a} + e^{ik'_y a} + e^{-ik'_y a} \right) \\
&= \sum_{\mathbf{k}} a_{\mathbf{k}}^\dagger a_{\mathbf{k}} \left[\cos(k_x a) + \cos(k_y a) \right].
\end{aligned} \tag{32}$$

In a similar way one can show that $\sum_{\langle ij\rangle} a_i^\dagger a_i = \sum_{\mathbf{k}} 2 a_{\mathbf{k}}^\dagger a_{\mathbf{k}}$. Leaving out the constant terms, our linearized spin wave Hamilationian now takes the form

$$\begin{aligned}
H \;&=\; 2SJ \sum_{\mathbf{k}} \left(2 - \cos(k_x a) - \cos(k_y a)\right) a_{\mathbf{k}}^\dagger a_{\mathbf{k}} \\
&= \sum_{\mathbf{k}} \omega_{\mathbf{k}} a_{\mathbf{k}}^\dagger a_{\mathbf{k}}\,,
\end{aligned} \tag{33}$$

from which the dispersion relation follows:

$$\omega_{\mathbf{k}} = \; 2SJ \left(2 - \cos(k_x a) - \cos(k_y a)\right). \tag{34}$$

Approximating for small k, we find exactly the same quadratic dispersion as we did in Eq.(24):

$$\omega_k \;\simeq\; SJ \left((k_x a)^2 + (k_y a)^2\right) \;= SJ \left(\mathbf{k}a\right)^2, \qquad (k_x a, k_y a \ll 1). \tag{35}$$

3.4 Thermodynamic properties

It is worth pointing out that our Hamiltonian, Eq.(33), shows resemblance to the Hamiltonian of the harmonic oscillator:

$$H = \omega a^\dagger a\,, \tag{36}$$

where we ignored the ground state energy and where $a^\dagger$ and a are creation and annihilation operators of the harmonic oscillator, raising and lowering the total

energy by one quantum, $\hbar\omega$, respectively. Analogously, the magnon creation and annihilation operators raise and lower the total energy of the system by an amount $\epsilon_{\mathbf{k}} = \hbar\omega_{\mathbf{k}}$, which is precisely the energy of a magnon with wave vector $\mathbf{k}$.

We are now in a position to find the distribution function for magnons by writing down the partition function Z:

$$Z = \prod_{\mathbf{k}} Z_{\mathbf{k}} = \prod_{\mathbf{k}} \sum_{n=0}^{\infty} e^{-\beta n \hbar\omega_{\mathbf{k}}} = \prod_{\mathbf{k}} \frac{1}{1 - e^{-\beta\hbar\omega_{\mathbf{k}}}}. \tag{37}$$

The total energy E of the system is then given by

$$E = -\frac{\partial}{\partial\beta} \ln Z = -\frac{\partial}{\partial\beta} \sum_{\mathbf{k}} \ln\left(\frac{1}{1 - e^{-\beta\hbar\omega_{\mathbf{k}}}}\right) = \sum_{\mathbf{k}} \frac{1}{e^{\beta\hbar\omega_{\mathbf{k}}} - 1} \hbar\omega_{\mathbf{k}} \tag{38}$$

$$= \sum_{\mathbf{k}} \langle n_{\mathbf{k}} \rangle \hbar\omega_{\mathbf{k}}. \tag{39}$$

From this expression we immediately derive that the distribution function for magnons is given by

$$\langle n_{\mathbf{k}} \rangle = \frac{1}{e^{\beta\hbar\omega_{\mathbf{k}}} - 1}, \tag{40}$$

which is known as the Planck distribution.

As we have been treating magnons as bosons, let us compare Eq.(40) with the Bose-Einstein distribution function, Eq.(9). Evidently, since $\epsilon_{\mathbf{k}} = \hbar\omega_{\mathbf{k}}$, the chemical potential μ must be equal to zero when the system is in equilibrium. This also follows from the fact that, in the case of magnons, the total particle number is not conserved. Magnons can be excited and subsequently dissipated again as a consequence of interactions with phonons in the lattice. This process is being referred to as spin-lattice relaxation [8].

We saw in Paragraph 2.1 that, in order to reach a state of Bose-Einstein condensation, the chemical potential μ must be equal to the single-particle ground state energy. Since the single particle ground state energy of magnons is greater than zero, as we will see in more detail in the following section, there is no way for the system to reach Bose-Einstein condensation as long as it is in thermal equilibrium. However, when the particle density is increased, the chemical potential will increase as well, which gives rise to the possibility of creating a quasi-equilibrium state with non-zero chemical potential by pumping magnons into the system. These added magnons will experience magon-magnon interactions, thereby thermalizing into quasi-equilibrium. As long as these magnon-magnon interactions conserve the number of magons and the thermalization time is much shorter than the time it takes to reach true thermal equilibrium again, the system will remain in a steady quasi-equilibrium for a while [2, 8]. In this temporary situation it can be described by the Bose-Einstein distribution function with non-zero chemical potential. If the increased particle density exceeds the critical density N_c, thereby causing the chemical potential to reach the value of the single particle ground state energy, Bose-Einstein condensation can in principle be achieved.

4 Bose-Einstein condensation of magnons: experimental observation

In the previous section we found the conditions under which magnon Bose-Einstein condensation could theoretically occur. Quasi-equilibrium Bose-Einstein condensation of magnons, however, is not only a theoretical phenomenon, but has actually been observed experimentally. In this section we will discuss the concerning experiment in terms of background, set up and results.

4.1 Background of the experiment

In 2006 the experimental observation of quasi-equilibrium Bose-Einstein condenstion of magnons at room temperature was reported by Demokritov *et al.* [1]. Although Bose-Einstein condensation of magnons and other quasi-particles had been observed before, these observations had always been made at or below cryogenic temperatures. The extremely low temperatures were needed in order to decrease the critical density sufficiently to experimentally achievable values [2].

The main factor that made the new observation of Bose-Einstein condensation at room temperatures possible was the use of YIG as the material on which the experiments were performed. YIG is a ferrimagnetic material with a complicated lattice structure. Under the conditions of the experiment it can be considered as an effective ferromagnet, with lattice constant $a = 12.376$ Å [9]. What makes this material particularly suitable for experiments on magnon Bose-Einstein condensation is the weak spin-lattice relaxation and, consequently, long magnon mean lifetime, exceeding 1000 ns [2]. The spin-lattice relaxtion time, i.e. the time it takes for the system to reach thermal equilibrium, is much longer than the thermalization time to reach quasi-equilibrium through magnon-magnon interactions, the latter being of the order of 100 ns [2].

In addition, YIG allows for the density of the magnon gas to be controlled and increased by means of parametric pumping [2], in which the energy of a microwave electromagnetic field is transferred to the system, causing the excitation of magnons. The distribution of the magnons over different energies can then be measured by applying Brillouin light scattering spectroscopy.

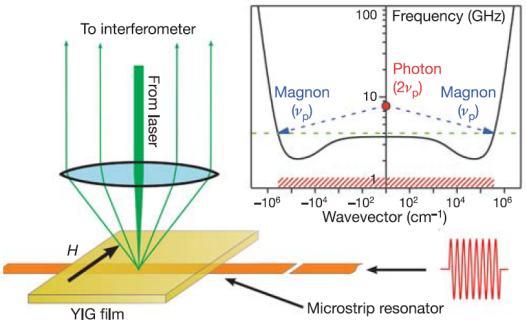

Figure 2: Set-up of the experiment and dispersion relation. Taken from Ref.[1]).

4.2 Experimental set-up

The material used in the experiments consists of thin YIG films of 2-10 micrometer thickness. An external magnetic field H, up to 1 kOe, is then applied parallel to the film. This causes the magnon frequency ν (related to the energy ϵ by $\epsilon = \hbar\omega = h\nu$) to have a nonzero minimum at 2-3 GHz [1]. Through parametric pumping the magnon density can be increased by 10^{19} cm^{-3}, which allows for a sufficient increase of μ to take on the value of the minimal energy [1]. As shown in Figure 2 a laser beam is focused onto a resonator situated underneath the YIG film. The beam passes trough the film, is reflected by the resonator and passes through the film again, before being sent to an interferometer for frequency analysis of photons scattered by magnons [1]. The dispersion relation is also displayed in the figure and shows two degenerate minima at wavevector magnitude $k = 5 \times 10^4 \text{cm}^{-1}$.The energy minimum corresponds to a frequency of 2.1 GHz.

4.3 Results and interpretation

In order to draw any conclusions about wether the system reaches a state of Bose-Einstein condensation, the measured scattering intensity as a function of frequency, $I(\nu)$, needs to be related to the occupation function $n(\nu)$ describing the magnon distribution over frequencies. This occupation function is just the Bose-Einstein distribution function:

$$n(\nu) \;=\; \frac{1}{e^{\beta(h\nu-\mu)}-1}. \tag{41}$$

Theoretically the intensity is proportional to the spectral density of the magnons, $I(\nu) \sim D(\nu)n(\nu)$, where $D(\nu)$ is the density of states. If $D(\nu)$ is known, the measured spectra can thus be interpreted by matching them to $n(\nu)$. In order to find an expression for $D(\nu)$ the authors measured the scattering intensities without pumping, i.e. with the system being in thermal equilibrium and μ equal to zero. The occupation function is then just the Planck distribution function:

$$n(\nu) \;=\; \frac{1}{e^{\beta h\nu}-1}. \tag{42}$$

The spectrum measured under these circumstances was used to find a fit of $D(\nu)$. The result of this fit is shown in Figure 3 by the dashed line. This functiun $D(\nu)$ was subsequently used to fit the measured spectra at different delay times to the occupation function (Eq.(41)), i.e. the Bose-Einstein distribution function, with the chemical potential μ as a fitting parameter. It was shown that for a delay time of 300 ns the experimental data could be fitted very well to the Bose-Einstein distribution function, with μ approaching the energy minimum. This indicates that the magnons had by that time thermalized into a quasi-equilibrium state. For delay times of 400 and 500 ns, however, the data could not be described by Bose-Einstein statistics, due to a high and narrow peak at the frequency minimum [1]. The width of this peak was five orders of magnitude smaller than a normal thermal distribution [2]. This was interpreted as a strong indication that the increased magnon density had exceeded the critical value and a Bose-Einstein condensate had been formed.

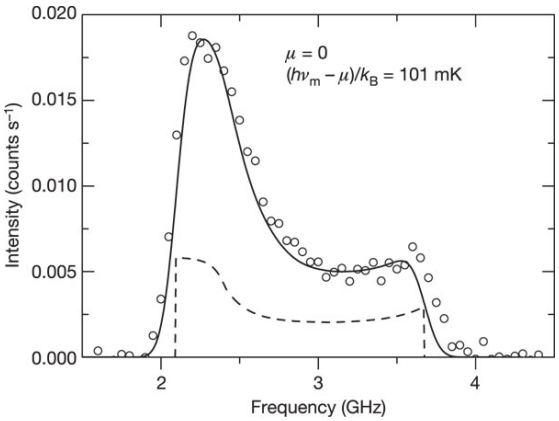

Figure 3: The density of states $D(\nu)$, obtained from the fit, is shown by the dashed line. Taken from Ref.[1].

5 Density of states: a theoretical approach

So far we have encountered the density of states a couple of times and we found out that it plays a crucial role in relating the distribution function to the particle density. For that same reason it was required at the previously discussed experiment in order to interpret the measured spectral intensities in terms of occupation numbers, leading to the conclusion that, at some point, Bose-Einstein statistics could no longer account for the large number of magnons around the single-particle ground state, which was considered proof for the observation of Bose-Einstein condensation. What is slightly curious, is the fact that the authors did not actually calculate the density of states, neither analytically nor numerically, but obtained it in the form of a fit function, by fitting the data to the Planck distribution function. In this section we will try to derive an expression for the density of states by taking on a theoretical approach, considering a specific model for magnon interactions in YIG. We will first derive the dispersion relation, which will subsequently allow us to calculate the density of states.

5.1 A model for magnons in YIG

We saw before that the density of states can be calculated once the dispersion relation is known, so in order to obtain the dispersion relation with sufficient accuracy, a theoretical model for magnons in YIG, corresponding to the situaton in the experiment, is required. Such a model has been used by serveral authors before [9, 10, 11], either in order to provide a theoretical basis and understanding for interpreting experimental results, such as the specific magnon dispersion with two degenerate minima as depicted in Figure 2, or in order to desribe transport of magnons in YIG and calculate related quantities such as the resistivity and relaxation time [8]. As mentioned before, YIG has a complicated cubic lattice structure with ferrimagnetic ordering. In the long wavelength limit, which is accurate for the energy scales relevant to the experiment, it can be modeled as a Heisenberg ferromagnet with an effective spin $S = 14.2$. In section 3 we already encountered the simplest form of the Heisenberg Hamiltionian, Eq.(17).

In order to get a more realistic description of the magnon energies, we will now include dipole-dipole interactions, as well as the Zeeman term associated with the external magnetic field $\mathbf{H}_e$. The Hamiltonian will then take the form [9, 8]

$$H = -F\sum_m S_m^z - \frac{1}{2}\sum_{m,n}\sum_{\alpha,\beta}\left[J_{mn}\delta_{\alpha,\beta} + D_{mn}^{\alpha\beta}\right]S_m^\alpha S_n^\beta, \tag{43}$$

where m and n label the lattice sites and $F = \mu H_e$, where $\mu = g\mu_B$ is the magnetic moment and $\mathbf{H}_e = H_e\hat{\mathbf{e}}_z$ is the external magnetic field which we choose to point along the z-direction. The exchange coupling $J_{mn} = J$ for nearest neighbours and zero otherwise. The dipolar tensor is given by [9]

$$D_{mn}^{\alpha\beta} = (1-\delta_{m,n})\frac{\mu^2}{|\mathbf{r}_{mn}|^3}\left[3\hat{\mathbf{r}}_{mn}^\alpha\hat{\mathbf{r}}_{mn}^\beta - \delta_{\alpha,\beta}\right], \tag{44}$$

where $\mathbf{r}_{mn} = \mathbf{r}_m - \mathbf{r}_n$ with $\mathbf{r}_m$ denoting the position vector of lattice site m. The geometry of the experiment is shown schematically in Figure 3, and allows for the approximation of an infinite length and width w of the film, compared to the thickness d, which is several micrometers and therefore covers several thousands of lattice sites in the x-direction, with a being equal to 12.376 Å.

In the classical ground state all spins point along the magnetic field in the z-direction. Analogously to what we did in section 3, we can now describe small fluctuations from the ground state orientation by means of bosonic operators representing magnons. We will again use the Holstein-Primakoff transformation and expand the Hamiltonian, Eq.(43), in terms of the bosonc operatrs a and $a^\dagger$, given in Eq.(26). The expansion in powers of $1/S$ is justified here since the effective spin S is quite large [9]. In this way the Hamiltonian can be written as [8]

$$H = H_0 + H_2 + H_3 + H_4 + \cdots, \tag{45}$$

where the subscripts denote the order in boson operators, which is equivalent to the order of magnon-magnon interaction. The quadratic part of the Hamiltonian will then take the form [8]

$$H_2 = \sum_{m,n}\left[A_{mn}a_m^\dagger a_n + \frac{1}{2}B_{mn}a_m a_n + \frac{1}{2}B_{mn}^* a_m^\dagger a_n^\dagger\right], \tag{46}$$

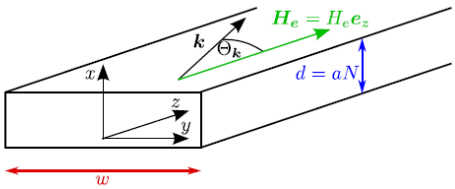

Figure 4: Geometry of the system. Taken from Ref.[9].

where

$$A_{mn} = F\delta_{m,n} - S\left[J_{mn} - \delta_{m,n}\sum_l J_{ml}\right] + S\left[\delta_{m,n}\sum_l D^{zz}_{ml} - \frac{1}{2}(D^{xx}_{mn} + D^{yy}_{mn})\right], \tag{47}$$

and

$$B_{mn} = -\frac{S}{2}\left[D^{xx}_{mn} - 2iD^{xy}_{mn} - D^{yy}_{mn}\right]. \tag{48}$$

It is the quadratic part of H from which the dispersion relation follows [8]. In order to obtain the dispersion relation we first need to Fourier transform H_2 to momentum space. Since the YIG film can be considered infnitely long in the z- and y-directions, we can use translational invariance along these directions and perform a Fourier transform as usual. The x-direction is obviously not infinite and therefore translational invariance along this direction cannot be assumed without loss of accuracy [9]. In the long wavelength limit, however, the thickness d of the film is of the same order of magnitude as the typical wavelength, allowing for an approximation that treats the system as practically two dimensional. In this approximation translational invariance wih periodic boundary conditions is assumed in all three directions, after which the x-component of the wave vector, k_x, is set to zero [9]. The following Fourier transforms are used [8]:

$$a_m = \frac{1}{\sqrt{N}}\sum_{\mathbf{k}} a_{\mathbf{k}} e^{i\mathbf{k}\cdot\mathbf{r}_m}, \tag{49}$$

$$A_{mn} = \frac{1}{N}\sum_{\mathbf{k}} A_{\mathbf{k}} e^{i\mathbf{k}\cdot\mathbf{r}_{mn}}, \tag{50}$$

$$B_{mn} = \frac{1}{N}\sum_{\mathbf{k}} B_{\mathbf{k}} e^{i\mathbf{k}\cdot\mathbf{r}_{mn}}. \tag{51}$$

Substituting these into Eq.(46) yields [9]:

$$H_2 = \sum_{\mathbf{k}}\left[A_{\mathbf{k}} a^\dagger_{\mathbf{k}} a_{\mathbf{k}} + \frac{1}{2}B_{\mathbf{k}} a_{-\mathbf{k}} a_{\mathbf{k}} + \frac{1}{2}B^*_{\mathbf{k}} a^\dagger_{-\mathbf{k}} a^\dagger_{\mathbf{k}}\right]. \tag{52}$$

Expressions for $A_{\mathbf{k}}$ and $B_{\mathbf{k}}$ are obtained by evaluating the Fourier transforms of the dipolar terms and exchange coupling in Eq.(47) and Eq.(48). The sums over lattice sites in all three directions are converted to integrals by the substitution

$$\sum_{x_i}\sum_{y_i}\sum_{z_i} \to \frac{1}{a^3}\int_{-d/2}^{d/2} \mathrm{d}x \int \mathrm{d}y \int \mathrm{d}z\,. \tag{53}$$

This eventually yields [9]

$$J_{\mathbf{k}} = 2J\left[\cos(k_y a) + \cos(k_z a)\right]; \tag{54}$$

$$D^{xx}_{\mathbf{k}} = \frac{4\pi\mu^2}{a^3}\left[\frac{1}{3} - f_{\mathbf{k}}\right]; \tag{55}$$

$$D^{yy}_{\mathbf{k}} = \frac{4\pi\mu^2}{a^3}\left[\frac{1}{3} + \sin^2(\theta_{\mathbf{k}})(f_{\mathbf{k}} - 1)\right]; \tag{56}$$

$$D^{yy}_{\mathbf{k}} = \frac{4\pi\mu^2}{a^3}\left[\frac{1}{3} + \cos^2(\theta_{\mathbf{k}})(f_{\mathbf{k}} - 1)\right]; \tag{57}$$

$$D^{xy}_{\mathbf{k}} = 0\,, \tag{58}$$

where $f_{\mathbf{k}}$ is the form factor, given by

$$f_{\mathbf{k}} = \frac{1 - e^{-kd}}{kd}, \tag{59}$$

with $k = |\mathbf{k}|$, and where $\theta_{\mathbf{k}}$ is the angle between the wave vector $\mathbf{k}$ and the external magnetic field $\mathbf{H}_e$, such that

$$\mathbf{k} = k(\cos\theta_{\mathbf{k}}\hat{\mathbf{e}}_z + \sin\theta_{\mathbf{k}}\hat{\mathbf{e}}_y). \tag{60}$$

This leads to the following expressions:

$$A_{\mathbf{k}} = F + 4SJ - 2SJ[\cos(k_y a) + \cos(k_z a)] - \frac{\Delta}{2}\left[\sin^2\theta_{\mathbf{k}}(f_{\mathbf{k}} - 1) - f_{\mathbf{k}}\right], \tag{61}$$

$$B_{\mathbf{k}} = \frac{\Delta}{2}\left[\sin^2\theta_{\mathbf{k}}(f_{\mathbf{k}} - 1) + f_{\mathbf{k}}\right], \tag{62}$$

where the characteristic magnon energy due to dipolar interactions is given by

$$\Delta = \frac{4\pi\mu^2 S}{a^3}. \tag{63}$$

Noticing that $A_{\mathbf{k}}$ and $B_{\mathbf{k}}$ are both symmetric in $\mathbf{k}$, we can write Eq.(52) as

$$H_2 = \sum_{\mathbf{k}>0}\left[A_{\mathbf{k}}a^\dagger_{\mathbf{k}}a_{\mathbf{k}} + A_{\mathbf{k}}a^\dagger_{-\mathbf{k}}a_{-\mathbf{k}} + B_{\mathbf{k}}a_{-\mathbf{k}}a_{\mathbf{k}} + B^*_{\mathbf{k}}a^\dagger_{-\mathbf{k}}a^\dagger_{\mathbf{k}}\right]. \tag{64}$$

In order to diagonalize H_2, which means writing it in terms independent of bosonic operators and terms containing only number operators, which are of the form $b^\dagger_{\mathbf{k}}b_{\mathbf{k}}$, where b and $b^\dagger$ denote the boson annihilation and creation operators, we have to perform a Bogoliubov transformation [8, 10]. Details on this procedure can be found in the appendix. We introduce the new bosonic operators $b_{\mathbf{k}}$ and $b^\dagger_{\mathbf{k}}$ in terms of which the old ones can be expanded:

$$a_{\mathbf{k}} = u^*_{\mathbf{k}}b_{\mathbf{k}} - v_{\mathbf{k}}b^\dagger_{-\mathbf{k}}\,, \qquad a^\dagger_{-\mathbf{k}} = u_{\mathbf{k}}b^\dagger_{-\mathbf{k}} - v^*_{\mathbf{k}}b_{\mathbf{k}}\,, \tag{65}$$

where the condition $|u_{\mathbf{k}}|^2 - |v_{\mathbf{k}}|^2 = 1$ is imposed in order to make the new operators obey the bosonic commutation relation, $[b_{\mathbf{k}}, b^\dagger_{\mathbf{k}'}] = \delta_{\mathbf{k},\mathbf{k}'}$. Substituting

these relations into Eq.(64) gives [10]

$$H_2 = \sum_{\mathbf{k}>0} \left[\hbar\omega_{\mathbf{k}} (b^\dagger_{\mathbf{k}} b_{\mathbf{k}} + b^\dagger_{-\mathbf{k}} b_{-\mathbf{k}} + 1) - A_{\mathbf{k}} \right] \tag{66}$$

$$= \sum_{\mathbf{k}} \left[\hbar\omega_{\mathbf{k}} b^\dagger_{\mathbf{k}} b_{\mathbf{k}} + \frac{1}{2}(\hbar\omega_{\mathbf{k}} - A_{\mathbf{k}}) \right], \tag{67}$$

where

$$u_{\mathbf{k}} = \sqrt{\frac{A_{\mathbf{k}} + \hbar\omega_{\mathbf{k}}}{2\hbar\omega_{\mathbf{k}}}}, \qquad v_{\mathbf{k}} = \sqrt{\frac{A_{\mathbf{k}} - \hbar\omega_{\mathbf{k}}}{2\hbar\omega_{\mathbf{k}}}}, \tag{68}$$

and the dispersion is given by

$$\epsilon_{\mathbf{k}} = \hbar\omega_{\mathbf{k}} = \sqrt{A^2_{\mathbf{k}} - B^2_{\mathbf{k}}} = \sqrt{(A_{\mathbf{k}} - B_{\mathbf{k}})(A_{\mathbf{k}} + B_{\mathbf{k}})}. \tag{69}$$

Since we are considering the long wavelength limit, we can approximate Eq.(61) for small wave vectors, i.e. $ka \ll 1$, which gives

$$A_{\mathbf{k}} - B_{\mathbf{k}} = F + SJa^2k^2 - \Delta \sin^2\theta_{\mathbf{k}} (f_{\mathbf{k}} - 1), \tag{70}$$

$$A_{\mathbf{k}} + B_{\mathbf{k}} = F + SJa^2k^2 + \Delta f_{\mathbf{k}}. \tag{71}$$

We have thus obtained the dispersion relation as a function of k and $\theta_{\mathbf{k}}$, which indicates that the energy depends not only on the magnitude of the wave vector $\mathbf{k}$, which was the case in Eq.(35), but also on the direction of propagation. Comparing the dispersion in Eq.(69) with the one in Eq.(35), that followed from the simple Heisenberg Hamiltonian in which only exchange interactions were considered, we see that including the dipole-dipole interactions has substantially complicated the dispersion relation. Moreover, the dispersion mimimum is no longer at $\mathbf{k} = 0$, but, due to the competition between the long-range dipole-dipole interactions and the exchange interactions, working on short distances [9] the dispersion now shows a two-fold degenerate minimum at wave vector $\mathbf{k} = \mathbf{k}_0 = \pm k_0 \hat{\mathbf{e}}_z$. It is not too hard to derive from the above expressions that in the mimima $\theta_{\mathbf{k}} = 0$, i.e. $k_y = 0$. In the following paragraph we will try to find an expression for k_0 which will allow us to aproximate the dispersion around the two minima, thereby providing a way to obtain the density of states for energies close to the minimum $\epsilon_{\mathbf{k}_0} = \hbar\omega_{\mathbf{k}_0}$.

5.2 Obtaining the density of states

Now that we have found the dispersion relation, we can in principle compute the density of states. Unfortunately the dispersion is quite complicated and does not exhibit a trivial symmetry, unlike the quadratic dispersion in Eq.(35), which is spherically symetric in k-space. Therefore, we will have to compute the density of states numerically. We can, however, start by considering the low energy limit and approximate the dispersion around the energy minimum, which allows for an analytical computation of the corresponding density of states. Before we proceed with that, we will first rewrite the dispersion relation in terms of the

following dimensionless quantities:

$$\tilde{\epsilon}_{\tilde{\mathbf{k}}} = \frac{\hbar\omega_{\tilde{\mathbf{k}}}}{F}\,, \qquad |\tilde{\mathbf{k}}| = \tilde{k} = ka\,, \qquad \tilde{\Delta} = \frac{\Delta}{F}\,, \qquad \tilde{J} = \frac{SJ}{F}\,, \qquad \tilde{d} = \frac{d}{a}\,, \tag{72}$$

so that it takes the form

$$\tilde{\epsilon}_{\tilde{\mathbf{k}}} \;=\; \sqrt{\left(1 + \tilde{J}\tilde{k}^2 - \tilde{\Delta}\sin^2\theta_{\tilde{\mathbf{k}}}(f_{\tilde{\mathbf{k}}} - 1)\right)\,\left(1 + \tilde{J}\tilde{k}^2 + \tilde{\Delta}f_{\tilde{\mathbf{k}}}\right)}\,, \tag{73}$$

with

$$f_{\tilde{\mathbf{k}}} \;=\; \frac{1 - e^{-\tilde{k}\tilde{d}}}{\tilde{k}\tilde{d}}. \tag{74}$$

These dimensionless quantities serve to make later calculations more tractable and, additionally, their values will be easy to estimate as they are nothing but ratios between parameters of the system.

Low energy limit

The experiment was conducted at room temperature whereas the critical temperature for ferrimagnetic ordering in YIG is around 560 K. Therefore, the magnon energy will be relatively low and a large fraction of the magnons will already occupy the energy levels close to the ground state [8]. For that reason it makes sense to look more closely at the low energy regime of the dispersion relation. Approximating Eq.(73) around the two minima gives

$$\tilde{\epsilon}_{\tilde{\mathbf{k}}} \;\simeq\; \frac{\hbar^2}{2m_{\parallel}}(\tilde{k}_z \pm \tilde{k}_0)^2 \;+\; \frac{\hbar^2}{2m_{\perp}}\tilde{k}_y^2 \;+\; \tilde{\epsilon}_{\tilde{\mathbf{k}}_0}, \tag{75}$$

where

$$m_{\parallel} = \hbar^2\left(\frac{\partial^2\tilde{\epsilon}_{\tilde{\mathbf{k}}}}{\partial\tilde{k}_z^2}\bigg|_{\tilde{\mathbf{k}}=\tilde{\mathbf{k}}_0}\right)^{-1}, \qquad m_{\perp} = \hbar^2\left(\frac{\partial^2\tilde{\epsilon}_{\tilde{\mathbf{k}}}}{\partial\tilde{k}_y^2}\bigg|_{\tilde{\mathbf{k}}=\tilde{\mathbf{k}}_0}\right)^{-1}, \tag{76}$$

as follows straightforwardly from the definition of the Taylor series. We will now find the value of $\mathbf{k}_0$ from Eq.(73), but in order to do so, we will first obtain the values of the quantities in Eq.(72). From Ref.[9], we use that the saturation magnetization of YIG is given by

$$4\pi M_S = 1750\,\mathrm{G}, \tag{77}$$

and the exchange stiffness ρ_{ex} of long-wavelength spin waves by

$$\frac{\rho_{ex}}{\mu} \;=\; \frac{JSa^2}{\mu} \;=\; 5.17\times10^{-13}\,\mathrm{Oe\ m^2}. \tag{78}$$

The magnetic moment is $\mu = g\mu_B$ with the effective g-factor set equal to 2 and the Bohr magneton $\mu_B \simeq 9.274\times10^{-21}$ erg G^{-1}. We are using Gaussian units, which is common in the literature and which allows us to express the magnetic field either in Gauss or Oersted, since they have the same dimensions in this

unit system. We now use that

$$M_S \,=\, \frac{\mu S}{a^3}\, 10^{-6}\,\mathrm{G} = \frac{\Delta}{\mu} \qquad \text{and} \qquad F \,=\, \mu H_e, \tag{79}$$

with the external field H_e applied in the experiment being equal to 700 Oe. In addition, we will look at a film thickness $d \simeq 5\,\mu\mathrm{m}$. As stated before, the system has an effective spin $S = 14.2$ and lattice constant $a = 12.376$ Å. Putting this all together, we come to the following values:

$$\tilde{\Delta} \,\simeq\, 2.5\,, \qquad \tilde{J} \,\simeq\, 482\,, \qquad \tilde{d} \simeq 4 \times 10^4. \tag{80}$$

Substituting these into Eq.(73), setting $\theta_{\tilde{\mathbf{k}}}$ to zero, since k_y equals zero in the minimum of $\epsilon_{\mathbf{k}}$, and evaluating the minimum $\epsilon_{min} \equiv \epsilon_{\mathbf{k}_0}$ of the dispersion yields

$$\tilde{\epsilon}_{min} \,=\, 1.0673 \qquad \text{and} \qquad \tilde{k}_0 \,=\, 0.0068. \tag{81}$$

Translating this back to physical quantities we find

$$k_0 \,=\, \frac{\tilde{k}_0}{a} \,=\, 5.4 \times 10^6\,\mathrm{m}^{-1}, \tag{82}$$

$$\nu_{min} \,=\, \frac{\epsilon_{min}}{h} \,=\, \frac{\tilde{\epsilon}_{min} F}{h} \,=\, 2.09\,\mathrm{GHz}, \tag{83}$$

which is in agreement with [2] and where ν_{min} denotes the frequency corresponding to the energy minimum. We use our value of $\tilde{k}_0$ to evaluate explicitly the expressions in Eq.(76), which yields

$$m_{\parallel} \,=\, \frac{\hbar^2}{2826} \qquad m_{\perp} \,=\, \frac{\hbar^2}{54382}\,, \tag{84}$$

so that we can write Eq.(75) as

$$\tilde{\epsilon}_{\tilde{\mathbf{k}}} \,\simeq\, \alpha(\tilde{k}_z \pm \tilde{k}_0)^2 \,+\, \beta\, \tilde{k}_y^2 \,+\, \tilde{\epsilon}_{min}, \tag{85}$$

where $\alpha = 2826/2$ and $\beta = 54382/2$. Evidently, the curvature around the two minima is larger in the y-direction than in the z-direction. The shape of the dispersion as a function of k_z and k_y is shown in Figure 5(a), depicting the two degenerate minima at $\pm k_0$. We see that the curvature along the y-direction is larger indeed. As we are currently considering the small energy limit, i.e. the range of energy levels close to the ground state, we have to zoom in on one of the minima in the region where Eq.(85) actually has meaning. This is depicted in Figure 5(b), where the contour lines represent the energy levels. Taking the larger gradient along k_y into account, it is evident that the energy levels describe ellipses in k-space.

In order to find the density of states in this region, we can use the geometry of the respective k-space, i.e. the elliptical shape of each energy level. Defining

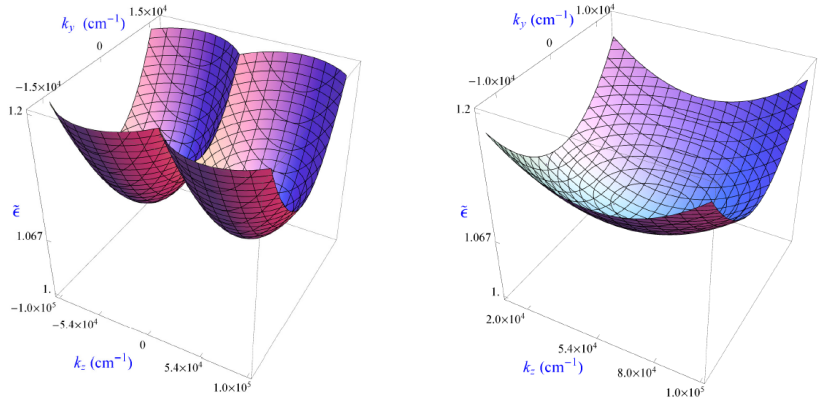

(a) (b)

Figure 5: Plots of the dispersion approximated around the energy minimum. In (a) the two minima at $k_z = \pm 5.4 \times 10^4$ cm^{-1} are clearly visible. In (b) we zoomed in on the minimum at $k_z = 5.4 \times 10^4 \text{cm}^{-1}$, covering the region appropriate within the approximation.

$E_{\mathbf{k}} \equiv \tilde{\epsilon}_{\mathbf{k}} - \tilde{\epsilon}_{min}$, we can write, from Eq.(85)

$$E_{\mathbf{k}} = \alpha\, a^2\, (k_z - k_0)^2 + \beta\, a^2\, k_y^2\,; \tag{86}$$

$$1 = \frac{\alpha}{E_{\mathbf{k}}}\, a^2\, (k_z - k_0)^2 + \frac{\beta}{E_{\mathbf{k}}}\, a^2\, k_y^2 \tag{87}$$

$$= \left(\frac{k_z - k_0}{\sqrt{E_{\mathbf{k}}/\alpha a^2}}\right)^2 + \left(\frac{k_y}{\sqrt{E_{\mathbf{k}}/\beta a^2}}\right)^2. \tag{88}$$

This is precisely the equation of an ellipse with semi-major axis $\sqrt{E_{\mathbf{k}}/\alpha a^2}$ and semi-minor axis $\sqrt{E_{\mathbf{k}}/\beta a^2}$. The area $S_{\mathbf{k}}$ of the ellipse corresponding to the energy $\tilde{\epsilon}_{\mathbf{k}}$ is then given by

$$S_{\mathbf{k}} = \pi \times \sqrt{E_{\mathbf{k}}/\alpha a^2} \times \sqrt{E_{\mathbf{k}}/\beta a^2} = \frac{\pi E_{\mathbf{k}}}{a^2\sqrt{\alpha\beta}}. \tag{89}$$

The number of states in the two dimensional k-space covered by an ellipse with area $S_{\mathbf{k}}$ is equal to this area divided by the area a single state makes up in k-space. Taking a look at Figure 5(b) again, we readily see that this corresponds to the number of states with energy $\leq \tilde{\epsilon}_{\mathbf{k}}$. However, for each energy level $\tilde{\epsilon}_{\mathbf{k}}$ there are two ellipses contributing to the number of states, one around each of the two minima. The total number of states $\tilde{n}(\tilde{\epsilon}_{\mathbf{k}})$ per unit area in normal space is then given by:

$$\tilde{n}(\tilde{\epsilon}_{\mathbf{k}}) = 2 \times \frac{1}{(2\pi)^2}\, \frac{\pi E_{\mathbf{k}}}{a^2\sqrt{\alpha\beta}} = \frac{1}{2\pi a^2\sqrt{\alpha\beta}}\, (\tilde{\epsilon}_{\mathbf{k}} - \epsilon_{min}), \tag{90}$$

or, dropping the subscript and writing the total number of states as a function of energy,

$$\tilde{n}(\tilde{\epsilon}) = \frac{1}{2\pi a^2\sqrt{\alpha\beta}}\, (\tilde{\epsilon} - \tilde{\epsilon}_{min}). \tag{91}$$

Converting this to the number of states as a function of the actual energy $\epsilon = F\tilde{\epsilon}$,

we obtain

$$n(\epsilon) \;=\; \frac{1}{2\pi F a^2\sqrt{\alpha\beta}}\,(\epsilon-\epsilon_{min}). \tag{92}$$

Since a negative number of states is unphysical, Eq.(92) only has meaning when $\epsilon \geq \epsilon_{min}$, reflecting the fact that there are no states to be occupied at energies smaller than the minimum magnon energy. Recalling the definition of the density of states as given in Eq.(16), we can write down the following expression for the density of states:

$$D(\epsilon) \;=\; \frac{\partial}{\partial\epsilon}n(\epsilon) \;=\; \begin{cases} \frac{1}{2\pi F a^2\sqrt{\alpha\beta}} & \epsilon \geq \epsilon_{min} \\ 0 & \epsilon \leq \epsilon_{min} \end{cases} \quad . \tag{93}$$

Hence, we have just found that the density of states in the low energy limit of our two dimensional system is a constant, i.e. it does not depend on the energy ϵ. Taking a look again at Figure 3, we see that the density of states obtained from the fit of the experimental data, is rather flat indeed, i.e. approximately constant, in the range of frequencies close to the frequency minimum of 2.1 GHz. So far our approximation seems to be in agreement with the result of the fit. Figure 3 furthermore shows a negative slope of the density of states for a range of frequencies around 2.5 GHz whereas for higher frequencies, corresponding to higher energies, the slope seems to be approximately zero again. We will now try to find the density of states from the complete dispersion relation, Eq.(73), that followed from the model for magnons in YIG.

Calculating the complete density of states

We have just seen that when the dispersion is approximated around the two minima, geometry can be used to find an expression for the density of states. Unfortunately this approach will not work when we consider the complete dispersion. In order to find the density of states, we will use the definition of the density of states given in Eq.(15), with the difference that we are now considering an effectively two dimensional system. Taking Eq.(73) as our dispersion, we then have

$$\tilde{D}(\tilde{\epsilon}) = \int \frac{\mathrm{d}\mathbf{k}}{(2\pi)^2}\;\delta(\tilde{\epsilon}-\tilde{\epsilon}_{\mathbf{k}}) \;=\; \frac{1}{(2\pi)^2}\int \mathrm{d}k\,k\int \mathrm{d}\theta_{\mathbf{k}}\,\delta(\tilde{\epsilon}-\tilde{\epsilon}_{\mathbf{k}}) \tag{94}$$

$$= \frac{1}{(2\pi)^2}\int \mathrm{d}k\,k\int \mathrm{d}\theta_{\mathbf{k}}\sum_i \left|\left(\frac{\mathrm{d}(\tilde{\epsilon}-\tilde{\epsilon}_{\mathbf{k}})}{\mathrm{d}\theta_{\mathbf{k}}}\bigg|_{\theta_{\mathbf{k}}=\theta_i}\right)^{-1}\right|\delta(\theta_{\mathbf{k}}-\theta_i)\,, \tag{95}$$

where the θ_i denote the solutions to the equation

$$\tilde{\epsilon}-\tilde{\epsilon}_{\mathbf{k}} = 0. \tag{96}$$

Working this out, we find for θ_i:

$$\sin^2\theta_i \;=\; \frac{1+\tilde{J}k^2a^2}{\tilde{\Delta}(f_{\mathbf{k}}-1)} - \frac{\tilde{\epsilon}^2}{(1+\tilde{J}k^2a^2+\tilde{\Delta}f_{\mathbf{k}})\tilde{\Delta}(f_{\mathbf{k}}-1)} \equiv G(k)\,, \tag{97}$$

where we introduced $G(k)$ for notational convenience. From Eq.(97) we see that there are four solutions for $0 \leq \theta_i \leq 2\pi$. We also find that

$$\left(\frac{\mathrm{d}(\tilde{\epsilon} - \tilde{\epsilon}_{\mathbf{k}})}{\mathrm{d}\theta_{\mathbf{k}}}\right)^{-1} = \frac{\tilde{\epsilon}_{\mathbf{k}}}{(1 + \tilde{J}k^2a^2 + \tilde{\Delta}f_{\mathbf{k}})\tilde{\Delta}(f_{\mathbf{k}} - 1)\sin\theta_{\mathbf{k}}\cos\theta_{\mathbf{k}}}. \tag{98}$$

Because we are interested in the absolute value of Eq.(98) when evaluated in θ_i, and because of goniometrical symmetry, we see that each of the four θ_i will contribute equally to the sum in Eq.(95). Therefore, we can write

$$\delta(\tilde{\epsilon} - \tilde{\epsilon}_{\mathbf{k}}) = \frac{4\tilde{\epsilon}}{(1 + \tilde{J}k^2a^2 + \tilde{\Delta}f_{\mathbf{k}})\tilde{\Delta}(1 - f_{\mathbf{k}})\sin\theta_o\cos\theta_o}\,\delta(\theta_{\mathbf{k}} - \theta_o)\,, \tag{99}$$

where

$$\theta_o = \arcsin\sqrt{G(k)}. \tag{100}$$

Substituting Eq.(99) into Eq.(95) and evaluating the integral over $\theta_{\mathbf{k}}$ yields

$$\frac{1}{(2\pi)^2}\int_0^\infty \mathrm{d}k\, k\, \frac{4\tilde{\epsilon}}{(1 + \tilde{J}k^2a^2 + \tilde{\Delta}f_{\mathbf{k}})\tilde{\Delta}(1 - f_{\mathbf{k}})\sin\theta_o\cos\theta_o}. \tag{101}$$

The integral over k is restricted, however, as a consequence of the implied condition Eq.(97) imposes on $G(k)$. It is evident that $0 \leq G(k) \leq 1$, which we can account for by adding two step functions that are defined by

$$\Theta(x) = \begin{cases} 1 & x > 0 \\ 0 & x < 0 \end{cases}. \tag{102}$$

In this way, we eventually obtain the following expression for the density of states

$$\tilde{D}(\tilde{\epsilon}) = \frac{4\tilde{\epsilon}}{(2\pi)^2}\int_0^\infty \mathrm{d}k\, k\, \frac{\Theta(G(k,\tilde{\epsilon}))\;\Theta(1 - G(k,\tilde{\epsilon}))}{(1 + \tilde{J}k^2a^2 + \tilde{\Delta}f_{\mathbf{k}})\tilde{\Delta}(1 - f_{\mathbf{k}})\sin\theta_o\cos\theta_o}. \tag{103}$$

This integral will have to be computed numerically, but this task is left for future work.

6 Conclusion

In this Thesis the density of states of a system of magnons in YIG was examined. The motivation for this came from the experimental observation of quasi-equilibrium Bose-Einstein condensation of magnons in YIG at room temperature, reported by Demokritov *et al.* in 2006 [1]. In order to understand this experiment, we first described what Bose-Einstein condensation actually is, by deriving the Bose-Einstein distribution function. This function is only applicable to bosons and describes the average occupation number for each energy state, labeled by the wave vector $\mathbf{k}$. We saw that when the chemical potential reaches the value of the lowest energy level, i.e. the single particle ground state energy, a macroscopic fraction of the total particle density will occupy this single particle ground state. This is what we call Bose-Einstein condensation. In

order for Bose-Einstein condensation to occur, the temperature must be lowered until it reaches a critical value, or the particle density must be increased until it reaches a critical value. We saw that the total particle number and density can be obtained by converting the summation of the distribution function over all wave vectors into an integral over the corresponding energy. In order to do this, however, the density of states is necessary and therefore has to be obtained first. The density of states relates the distribution function to the particle density.

Next, we took a closer look at the concept of magnons. We saw that magnons are quasiparticles that can be thought of as elementary excitations in the magnetization of magnetic materials. From a classical viewpoint they can be pictured as spin waves: small deviations of the spins from their ground state orientations, propagating through the material like waves. Because magnons behave like weakly interacting bosons as long as the temperature is small compared to the critical temperature for magnetic ordering of the material, they can quantum mechanically be described by bosonic operators following from a Holstein-Primakoff transformation. We considered the simple Heisenberg Hamiltonian which takes account of exchange interactions only, and expanded it in terms of these bosonic operators, which eventually yielded a quadratic dispersion relation, i.e. the energy turned out to be a function of the square of the wave vector.

In the experiment the total magnon density was increased by parametric pumping in order to achieve Bose-Einstein condensation. Since the total magnon number is not conserved, the chemical potential equals zero in thermal equilibrium and a Bose-Einstein condensate can only occur when the system is in quasi-equilibrium, a temporary state that lasts until the excited magnons relax into the lattice again. The experiment was conducted on YIG, a material very suitable since it allows for a long magnon lifetime. The measurements indicated that at some point the particle density around the ground state could no longer be described by the Bose-Einstein distribution function, which was interpreted as the occurrence of Bose-Einstein condensation. In order to interpret the results, the necessary density of states was obtained from a fit of the measured magnon spectrum without pumping, to the Bose-Einstein distribution function.

The aim of this Thesis was to find an expression for the density of states by taking on a theoretical approach. We therefore considered a specific model for magnons in YIG, taking account of the Zeeman energy, the exchange interactions and the dipole-dipole interactions. We treated the system as effectively two dimensional, for which we had to make the approximation of translational invariance in all three directions. We used the Holstein-Primakoff transformation again, which eventually yielded an expression for the dispersion relation. The dispersion turned out to be a function of both the norm of the wave vector, k, and the angle $\theta_{\mathbf{k}}$ between the wave vector and the external magnetic field. Since it is quite a complicated function, calculating the density of states from it is not a trivial task. We therefore approximated the dispersion around the minimum magnon energy, which we found to be two-fold degenerate at $k_z = \pm k = \pm 5.4 \times 10^4$ cm^{-1} and corresponding to a frequency of 2.1 GHz, which is in agreement with [1, 2]. We saw that the energy levels describe ellipses in k-space, which yields a density of states independent of the energy. This seems to be in agreement with the fitted density of states in the range of energies close the minimum. Eventually, we used the complete dispersion relation without further approximations, in order to find an expression for the

density of states. By rewriting the delta function in Eq.(94), and evaluating the integral over the angle $\theta_{\mathbf{k}}$, we obtained an expression for the density of states in the form of an integral over the norm of the wave vector, k. This integral will further have to be evaluated numerically, which is left for future work.

Appendix

Bogoliubov Transformation

In Paragraph 5.1 we briefly discussed a Bogoliubov transformation that was used to diagnolaize the Hamiltoninan in order to find the dispersion relation. Here we will see in more detail what this procedure encompasses.

We found the quadratic part of the Hamiltonian (Eq.(64)) to be of the form

$$H_2 = \sum_{\mathbf{k}>0} \left[A_{\mathbf{k}} a^\dagger_{\mathbf{k}} a_{\mathbf{k}} + A_{\mathbf{k}} a^\dagger_{-\mathbf{k}} a_{-\mathbf{k}} + B_{\mathbf{k}} a_{-\mathbf{k}} a_{\mathbf{k}} + B^*_{\mathbf{k}} a^\dagger_{-\mathbf{k}} a^\dagger_{\mathbf{k}} \right], \tag{104}$$

which we want to rewrite in such a way that it only contains constants and operators the form $b^\dagger_{\mathbf{k}} b_{\mathbf{k}}$, where b and $b^\dagger$ denote the boson annihilation and creation operators. Let us first rewrite the argument of the sum in Eq.(104) as

$$\begin{pmatrix} a^\dagger_{\mathbf{k}} & a^\dagger_{-\mathbf{k}} \end{pmatrix} \begin{pmatrix} A_{\mathbf{k}} & B_{\mathbf{k}} \\ B_{\mathbf{k}} & A_{\mathbf{k}} \end{pmatrix} \begin{pmatrix} a_{\mathbf{k}} \\ a^\dagger_{-\mathbf{k}} \end{pmatrix} - A_{\mathbf{k}}, \tag{105}$$

where we used that $a_{-\mathbf{k}} a^\dagger_{-\mathbf{k}} - 1 = a^\dagger_{-\mathbf{k}} a_{-\mathbf{k}}$. We see that the off diagonal matrix elements of the matrix in the middle in Eq.(105) are nonzero, which is precisely what we want to change. We therefore assume that there is another basis of bosonic operators, $b_{\mathbf{k}}$, $b_{-\mathbf{k}}$ and their hermitian conjugates, for which the matrix is diagonal, and we expand our operators $a_{\mathbf{k}}$, $a_{-\mathbf{k}}$ in this new basis:

$$a_{\mathbf{k}} = u_{\mathbf{k}} b_{\mathbf{k}} - v_{\mathbf{k}} b^\dagger_{-\mathbf{k}}\,, \qquad a^\dagger_{\mathbf{k}} = u_{\mathbf{k}} b^\dagger_{\mathbf{k}} - v_{\mathbf{k}} b_{-\mathbf{k}}\,; \tag{106}$$

$$a_{-\mathbf{k}} = u_{\mathbf{k}} b_{-\mathbf{k}} - v_{\mathbf{k}} b^\dagger_{\mathbf{k}}\,, \qquad a^\dagger_{-\mathbf{k}} = u_{\mathbf{k}} b^\dagger_{-\mathbf{k}} - v_{\mathbf{k}} b_{\mathbf{k}}\,, \tag{107}$$

where we chose the coefficients $u_{\mathbf{k}}$ and $v_{\mathbf{k}}$ to be real, for simplicity. One can check that this configuration preserves the bosonic commutation relations, $[b_{\mathbf{k}}, b^\dagger_{\mathbf{k}'}] = \delta_{\mathbf{k},\mathbf{k}'}$, in both bases, under the condition that $u^2 - v^2 = 1$, since

$$\begin{aligned} \left[a_{\mathbf{k}}, a^\dagger_{\mathbf{k}}\right] &= u^2_{\mathbf{k}} \left[b_{\mathbf{k}}, b^\dagger_{\mathbf{k}}\right] - u_{\mathbf{k}} v_{\mathbf{k}} \left[b_{\mathbf{k}}, b_{-\mathbf{k}}\right] - u_{\mathbf{k}} v_{\mathbf{k}} \left[b^\dagger_{-\mathbf{k}}, b^\dagger_{\mathbf{k}}\right] + v^2_{\mathbf{k}} \left[b^\dagger_{-\mathbf{k}}, b_{-\mathbf{k}}\right] && (108) \\ &= u^2_{\mathbf{k}} \left[b_{\mathbf{k}}, b^\dagger_{\mathbf{k}}\right] - v^2_{\mathbf{k}} \left[b_{-\mathbf{k}}, b^\dagger_{-\mathbf{k}}\right] = 1. && (109) \end{aligned}$$

We can now write the matrices in Eq.(105) in the following form:

$$\begin{pmatrix} a^\dagger_{\mathbf{k}} & a^\dagger_{-\mathbf{k}} \end{pmatrix} \begin{pmatrix} A_{\mathbf{k}} & B_{\mathbf{k}} \\ B_{\mathbf{k}} & A_{\mathbf{k}} \end{pmatrix} \begin{pmatrix} a_{\mathbf{k}} \\ a^\dagger_{-\mathbf{k}} \end{pmatrix} \tag{110}$$

$$= \begin{pmatrix} b^\dagger_{\mathbf{k}} & b_{-\mathbf{k}} \end{pmatrix} \begin{pmatrix} u_{\mathbf{k}} & -v_{\mathbf{k}} \\ -v_{\mathbf{k}} & u_{\mathbf{k}} \end{pmatrix} \begin{pmatrix} A_{\mathbf{k}} & B_{\mathbf{k}} \\ B_{\mathbf{k}} & A_{\mathbf{k}} \end{pmatrix} \begin{pmatrix} u_{\mathbf{k}} & -v_{\mathbf{k}} \\ -v_{\mathbf{k}} & u_{\mathbf{k}} \end{pmatrix} \begin{pmatrix} b_{\mathbf{k}} & b^\dagger_{-\mathbf{k}} \end{pmatrix} \tag{111}$$

$$= \begin{pmatrix} b^\dagger_{\mathbf{k}} & b_{-\mathbf{k}} \end{pmatrix} \begin{pmatrix} A_{\mathbf{k}}\left(u^2_{\mathbf{k}} + v^2_{\mathbf{k}}\right) - 2B_{\mathbf{k}} u_{\mathbf{k}} v_{\mathbf{k}} & B_{\mathbf{k}}\left(u^2_{\mathbf{k}} + v^2_{\mathbf{k}}\right) - 2A_{\mathbf{k}} u_{\mathbf{k}} v_{\mathbf{k}} \\ B_{\mathbf{k}}\left(u^2_{\mathbf{k}} + v^2_{\mathbf{k}}\right) - 2A_{\mathbf{k}} u_{\mathbf{k}} v_{\mathbf{k}} & A_{\mathbf{k}}\left(u^2_{\mathbf{k}} + v^2_{\mathbf{k}}\right) - 2B_{\mathbf{k}} u_{\mathbf{k}} v_{\mathbf{k}} \end{pmatrix} \begin{pmatrix} b_{\mathbf{k}} & b^\dagger_{-\mathbf{k}} \end{pmatrix}. \tag{112}$$

We now use that $u_{\mathbf{k}} - v_{\mathbf{k}} = 1$ in order to parameterize $u_{\mathbf{k}}$ and $v_{\mathbf{k}}$ [8]:

$$u_{\mathbf{k}} = \cosh t_{\mathbf{k}}\,, \qquad v_{\mathbf{k}} = \sinh t_{\mathbf{k}}\,. \tag{113}$$

This allows us to write $u^2+v^2 = \cosh 2t_{\mathbf{k}}$ and $2u_{\mathbf{k}}v_{\mathbf{k}} = \sinh 2t_{\mathbf{k}}$ (see, for example, Ref.[12]). Setting the off diagonal elements of the matrix in Eq.(112) to zero and solving for $u_{\mathbf{k}}$ and $u_{\mathbf{k}}$ eventually yields [12]

$$\begin{pmatrix} a_{\mathbf{k}}^\dagger & a_{-\mathbf{k}}^\dagger \end{pmatrix} \begin{pmatrix} A_{\mathbf{k}} & B_{\mathbf{k}} \\ B_{\mathbf{k}} & A_{\mathbf{k}} \end{pmatrix} \begin{pmatrix} a_{\mathbf{k}} \\ a_{-\mathbf{k}}^\dagger \end{pmatrix} \tag{114}$$

$$= \sqrt{A_{\mathbf{k}}^2 - B_{\mathbf{k}}^2}\, \left(b_{\mathbf{k}}^\dagger b_{\mathbf{k}} + b_{-\mathbf{k}}^\dagger b_{-\mathbf{k}} \right) + \sqrt{A_{\mathbf{k}}^2 - B_{\mathbf{k}}^2}\,. \tag{115}$$

Substituting this into our Hamiltonian, we arrive at

$$H_2 = \sum_{\mathbf{k}>0} \left[\sqrt{A_{\mathbf{k}}^2 - B_{\mathbf{k}}^2}\, \left(b_{\mathbf{k}}^\dagger b_{\mathbf{k}} + b_{-\mathbf{k}}^\dagger b_{-\mathbf{k}} \right) + \sqrt{A_{\mathbf{k}}^2 - B_{\mathbf{k}}^2} - A_{\mathbf{k}} \right] \tag{116}$$

$$= \sum_{\mathbf{k}} \left[\sqrt{A_{\mathbf{k}}^2 - B_{\mathbf{k}}^2}\, b_{\mathbf{k}}^\dagger b_{\mathbf{k}} + \frac{1}{2} \left(\sqrt{A_{\mathbf{k}}^2 - B_{\mathbf{k}}^2} - A_{\mathbf{k}} \right) \right] \tag{117}$$

$$= \sum_{\mathbf{k}} \left[\hbar\omega_{\mathbf{k}} b_{\mathbf{k}}^\dagger b_{\mathbf{k}} + \frac{1}{2} \left(\hbar\omega_{\mathbf{k}} - A_{\mathbf{k}} \right) \right], \tag{118}$$

which is indeed equal to the Hamiltonian in Eq.(67).

References

[1] S.O. Demokritov, V.E. Demidov, O. Dzyapko, G.A. Melkov, A.A. Serga, B. Hillebrands, and A.N. Slavin. Bose-Einstein condensation of quasi-equilibrium magnons at room temperature under pumping. *Nature* **443**, 430 (2006).

[2] O. Dzyapko, V.E. Demidov, S.O. Demokritov, G.A. Melkov, and A.N. Slavin. Direct observation of Bose-Einstein condensation in a parametrically driven gas of magnons. *New Journal of Physics* **9**, 64 (2007).

[3] H.T.C. Stoof, K.B. Gubbels, and D.B.M. Dickerscheid. *Ultracold quantum fields* (Springer, 2009).

[4] F. Bloch. Zur theorie des ferromagnetismus. *Zeitschrift fur Physik* **61**, 206 (1930).

[5] P. Norwik-Boltyk. Westfälische Wilhelms-Universität Münster. Bose-Einstein condensation of magnons observed directly in k-space. www.uni-muenster.de/Physik.Ap/Demokritov/en/Forschen/Forschungsschwerpunkte/mBECfnP.html (2012).

[6] M.G. Cottam, ed. *Linear and non-linear spin waves in magnetic films and superlattices* (World Scientific, 1994).

[7] D.I. Khomskii. *Basic aspects of the quantum theory of solids* (Cambridge University Press, 2010).

[8] A. Swaving. *Spin transport and dynamics in antiferromagnetic materials and magnetic insulators*, Ph.D. Thesis, Utrecht University (2012).

[9] A. Kreisel, F. Sauli, L. Bartosch, and P. Kopietz. Microscopic spin-wave theory for yttrium-iron garnet films. *The European Physical Journal B* **71**,59 (2009).

[10] J. Hick, F. Sauli, A. Kreisel, and P. Kopietz. Bose-Einstein condensation at finite momentum and magnon condensation in thin film ferromagnets. *The European Physical Journal B* **78**, 429 (2010).

[11] I.S. Tupitsyn, P.C.E. Stamp, and A.L. Burin. Stability of Bose-Einstein condensates of hot magnons in yttrium iron garnet films. *Physical Review Letters* **100**, 257202 (2008).

[12] J. Chalker. Quantum theory of condensed matter. Lecture notes, Oxford University (2012).